Journal of Solid State Chemistry 183 (2010) 1588–1594

Contents lists available at ScienceDirect

Journal of Solid State Chemistry

journal homepage: www.elsevier.com/locate/jssc

Metal diphosphonates with double-layer and pillared layered structures based on *N*-cyclohexylaminomethanediphosphonate

Yan-Hui Su, Deng-Ke Cao, Yan Duan, Yi-Zhi Li, Li-Min Zheng *

State Key Laboratory of Coordination Chemistry, Coordination Chemistry Institute, School of Chemistry and Chemical Engineering, Nanjing University, Nanjing 210093, PR China

ARTICLE INFO

Article history:
Received 15 February 2010
Received in revised form
5 May 2010
Accepted 8 May 2010
Available online 26 May 2010

Keywords:
Zinc
Cobalt
Manganese
N-cyclohexylaminomethanediphosphonic acid
Layer
Pillared layer
Antiferromagnetic interaction

ABSTRACT

Based on *N*-cyclohexylaminomethanediphosphonic acid ($cmdpH_4$), four new metal diphosphonate compounds with formula $M_3(cmdpH)_2(H_2O)_2$ [M=Zn(**1**), Co(**2**)] and $M_2(cmdpH_2)_2(4,4'\text{-bipy})_{0.5}(H_2O)$ [M=Co(**3**), Mn(**4**)] have been obtained and structurally determined. Compounds **1** and **2** are isostructural. Within the structure, the $M(2)O_6$ octahedra are each corner-shared with four PO_3C tetrahedra to form a single layer containing 3- and 7-member rings. Neighboring single layers are pillared by $M(1)O_4$ tetrahedra, resulting in a novel double-layer structure. The organic moieties of $cmdpH^{3-}$ are grafted on the two sides of the double layer. Compounds **3** and **4** are also isostructural, displaying a pillared layered structure. Within the inorganic layer, the $M(1)O_5$ tetragonal pyramids and $M(2)NO_5$ octahedra are each linked by PO_3C tetrahedra through corner-sharing, forming a layer in the *ab* plane which contains 3- and 10-member rings. These layers are pillared by 4,4′-bipyridine via coordination with the $M(2)$ atoms from the adjacent layers, leading to a three-dimensional open framework structure with channels generated along the *a*-axis. The organic groups of $cmdpH_2^{2-}$ locate within the channels. Magnetic studies show that antiferromagnetic interactions are dominant in compounds **2–4**. Field dependent magnetization reveals a spin flop behavior for **2**.

1. Introduction

Metal phosphonate chemistry has attracted increasing research attention due to their potential applications in catalysts [1–7], optics [8,9], sorptions [10–15] and magnetic materials [16–21]. In the category of phosphonate, diphosphonates play important roles in bone disorder treatments for their strong affinity to metal ions [22–24]. It is found that diphosphonate drugs possessing a nitrogen atom in the organic backbone behave high inhibition activity. Moreover, the studies show that both the positively charged nitrogen atom and the nature and the size of the substitute groups on nitrogen atom are crucial for the compound activity. However, it is not well understood why small modifications in their structures lead to significant alterations in their biological characteristics [25]. Thus the structure–activity relationship study is desired to understand diphosphonate physiological activity. In the viewpoint of coordination chemistry, investigation of versatile coordination modes of the nitrogen-containing diphosphonates to different metal ions would be helpful in better understanding the above mentioned problems of mechanism.

Matczak-Jon reviewed the supramolecular chemistry and complexation abilities of diphosphonates in solution or solid state [26]. It is noticed that structural reports on metal diphosphonates involving $(R_1)(R_2)NCH(PO_3H_2)_2$ ligands (Scheme 1) are rather limited thus far. Compound $Na_4[(O_3PCHN(CH_3)_2PO_3)W_2O_6]\cdot 11H_2O$ contains negatively charged chains made up of corner-sharing WO_6 octahedra and (dimethy1amino)methylenediphosphonate ($\mathbf{L}^1$) bridges. The Na^+ ions and water molecules locate in the space between the chains [27]. Based on aminomethylenediphosphonate ($\mathbf{L}^2$), $NaCo_2\{NH_3CH(PO_3)(PO_3H_{0.5})\}_2(H_2O)_2\cdot xH_2O$ was obtained showing an open framework structure in which the CoO_6 octahedra are bridged by PO_3C tetrahedra through vertex-sharing forming a layer containing 4- and 8-member rings. Neighboring layers are further connected by NaO_6 linkages [28]. While compound $Na_4Zn\{NH_3CH(PO_3)_2\}_2\cdot 4H_2O$ contains chains of $[Zn\{NH_3CH(PO_3)_2\}_2]_n^{4n-}$ made up of corner-sharing ZnO_6 octahedra and PO_3C tetrahedra, which are further connected by tetramers of edge-sharing NaO_6 octahedra. In the nickel compound $Ni\{NH_3CH(PO_3H)_2\}_2\cdot xH_2O$, a square-grid layer structure is found where the NiO_6 octahedra are corner-shared with PO_3C tetrahedra[29]. Apart from the transition metal compounds, lanthanide diphosphonates with 3D framework showing noninterpenetrated three-connected topology and 1D chain structure were also achieved through *N*-(2-pyridyl)-aminomethane-1,1-diphosphonic acid ($\mathbf{L}^3$) [30]. Clearly a slight change of the organic tails (R_1 or R_2) leads to structural diverse

* Corresponding author. Fax: +86 25 83314502.
E-mail addresses: lmzheng@nju.edu.cn, lmzheng@netra.nju.edu.cn (L.-M. Zheng).

0022-4596/$ - see front matter © 2010 Elsevier Inc. All rights reserved.
doi:10.1016/j.jssc.2010.05.008

because the methyl and hydrogen as well as pyridyl groups hold different sizes and functions in the construction of metal diphosphonates. To better understand the influences of the substitute groups on the structures and properties of metal diphosphonates, we introduce a flexible cyclohexyl group into iminomethylenediphosphonate. *N*-cyclohexylaminomethanediphosphonic acid [$C_6H_{11}NHCH(PO_3H_2)_2$, *cmdp*H_4, Scheme 2a] is synthesized subsequently, based on which four new metal-cmdp compounds with formula M_3(cmdpH)$_2$(H_2O)$_2$ [M=Zn(**1**), Co(**2**)] and M_2(cmdpH_2)$_2$(4,4-bpy)$_{0.5}$(H_2O) [M=Co(**3**), Mn(**4**)] are obtained. Compounds **1** and **2** show a novel double-layer structure, while compounds **3** and **4** exhibit a pillared layered structure. The magnetic properties of compounds **2–4** are also investigated.

2. Experimental section

2.1. Materials and methods

N-cyclohexylaminomethanediphosphonic acid [$C_6H_{11}NHCH(PO_3H_2)_2$, cmdpH_4] was prepared according to the literature method [31]. All the other starting materials were purchased commercially as reagent grade chemicals and used without further purification. The elemental analyses for C, H and N were performed in a PE240C elemental analyzer. The infrared spectra were recorded on a VECTOR 22 spectrometer with KBr pellets. Thermal analyses were performed in nitrogen with a heating rate of 10 °C/min on a TGA-DTA V1.1b Inst 2100 instrument. The powder XRD patterns were recorded on a Shimadzu XD-3A X-ray diffractometer. Magnetic susceptibility data of compounds **2–4** were obtained on microcrystalline samples (13.60 mg for **2**, 9.30 mg for **3** and 10.27 mg for **4**) using a Quantum Design MPMS-XL7 SQUID magnetometer. Diamagnetic corrections were made for both the sample holder and the compound estimated from Pascal's constants [32].

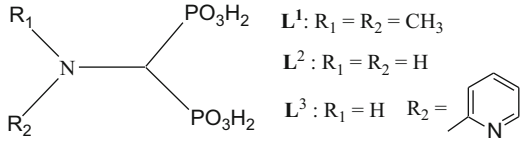

Scheme 1.

2.2. Syntheses

2.2.1. Synthesis of $Zn_3(cmdpH)_2(H_2O)_2$ (*1*)

A mixture of $ZnSO_4 \cdot 7H_2O$ (0.1 mmol, 0.0286 g), cmdpH_4 (0.1 mmol, 0.0310 g) and H_2O (8 cm^3), adjusted by 1 M NaOH to pH=2.5, was kept in a Teflon-lined autoclave at 140 °C for 72 h. After slow cooling to room temperature, the colorless lamellar crystals of compound **1** were collected as a monophasic material, judged by powder X-ray diffraction pattern. Yield: 60% based on Zn. Anal. Calcd. for $C_{14}H_{32}N_2O_{14}P_4Zn_3$: C, 21.75; H, 4.14; N, 3.62. Found: C, 20.74; H, 3.78; N, 3.46%. IR (KBr, cm^{-1}): 3439s, 3180m, 2935m, 2854m, 2554w, 1604m, 1458w, 1383m, 1114vs, 1066m, 968s, 775m, 556s. Thermal analysis reveals that the weight loss between 25 and 230 °C is 4.54%, in agreement with the removal of two coordinated water molecules (calcd. 4.66%).

2.2.2. Synthesis of $Co_3(cmdpH)_2(H_2O)_2$ (*2*)

Compound **2** was prepared in a similar way to that of **1** except that $CoSO_4 \cdot 7H_2O$ instead of $ZnSO_4 \cdot 7H_2O$ was used as the starting material and the pH of the reaction mixture was adjusted to 3.5. Purple lamellar crystals were obtained as a monophasic material, judged by powder X-ray diffraction pattern. Yield: 65% based on Co. Anal. Calcd. for $C_{14}H_{32}N_2O_{14}P_4Co_3$: C, 22.32; H, 4.28; N, 3.72. Found: C, 22.45; H, 4.64; N, 4.10%. IR (KBr, cm^{-1}): 3386br, 3180m, 2933m, 2856m, 2557w, 1608s, 1458w, 1383m, 1128vs, 1031m, 954s, 782m, 561s. Thermal analysis reveals that the weight loss between 25 and 260 °C is 4.78%, in agreement with the removal of two coordinated water molecules (calcd. 4.78%).

2.2.3. Synthesis of $Co_2(cmdpH_2)_2(4,4'\text{-bipy})_{0.5}(H_2O)$ (*3*)

Hydrothermal treatment of a mixture of $CoSO_4 \cdot 7H_2O$ (0.1 mmol, 0.0281 g), cmdpH_4 (0.1 mmol, 0.0310 g), 4,4′-bipyridine (0.1 mmol, 0.0156 g) and H_2O(8 cm^3), adjusted by 1 M NaOH to pH=3.2, at 180 °C for 48 h results in purple lamellar crystals of **3** as a monophasic material, judged by the powder X-ray diffraction pattern. Yield: 50% based on Co. Anal. Calcd. for $C_{19}H_{34}Co_2N_3O_{13}P_4$: C, 30.18; H, 4.79; N, 5.56. Found: C, 30.21; H, 4.67; N, 5.46%. IR (KBr, cm^{-1}): 3424br, 3024w, 2936m, 2855m,

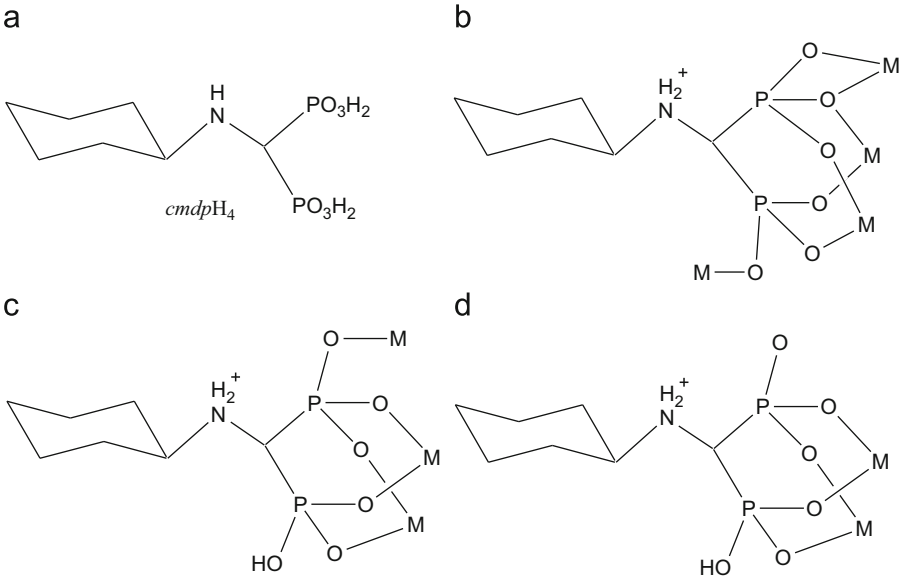

Scheme 2.

2804w, 2532w, 2454w, 1601m, 1497w, 1454m, 1382m, 1308m, 1211s, 1175s, 1141s, 1058vs, 1000s, 927m, 895m, 809m, 726m, 573m, 472m. Thermal analysis shows that the weight loss of 2.32% from 130 to 270 °C corresponds to the removal of one coordination water molecule, which is in good agreement with the calculated value (2.38%). Upon further heating, the continuous weight loss is observed, which corresponds to the decomposition of the compound.

2.2.4. Synthesis of $Mn_2(cmdpH_2)_2(4,4'\text{-bipy})_{0.5}(H_2O)$ (**4**)

Compound **4** was obtained as a single phase following a similar synthetic procedure to **3** except that $MnSO_4 \cdot H_2O$ instead of $CoSO_4 \cdot 7H_2O$ was used as the starting material. Yield: 50% based on Mn. Anal. Calcd. for $C_{19}H_{34}Mn_2N_3O_{13}P_4$: C, 30.50; H, 4.85; N, 5.62. Found: C, 30.85; H, 4.57; N, 5.53%. IR (KBr, cm^{-1}): 3461br, 3027w, 2933m, 2856m, 2539w, 1662w, 1602m, 1585m, 1531w, 1488m, 1455m, 1382m, 1317m, 1211s, 1178vs, 1139s, 1070vs, 997s, 935m, 894m, 808m, 719m, 574m, 470m. Thermal analysis confirms that the weight loss of 2.76% from 130 to 270 °C corresponds to the release of one coordination water molecule (calcd. 2.41%).

2.3. Crystallographic studies

Single crystals with dimensions $0.20 \times 0.12 \times 0.08\ mm^3$ for **1** and $0.28 \times 0.16 \times 0.08\ mm^3$ for **3** were selected for indexing and intensity data collection on a Bruker SMART APEX CCD diffractometer using graphite monochromatized Mo$K\alpha$ radiation ($\lambda = 0.71073$ Å) at room temperature. A hemisphere of data is collected in the θ range 2.25–25.99° for **1** and 1.84–26.00° for **3** using a narrow-frame method with scan widths of 0.30° in ω and exposure time of 15 s/frame. Numbers of observed and unique reflections are 6658 and 2559 ($R_{int} = 0.0484$) for **1**, 15,262 and 5635 ($R_{int} = 0.0385$) for **3**, respectively. The data were integrated using the Siemens SAINT program [33], with the intensities corrected for Lorentz factor, polarization, air absorption and absorption due to variation in the path length through the detector faceplate. Absorption corrections were applied. The structures were solved by direct methods and refined on F^2 by full matrix least squares using SHELXTL [34]. All non-hydrogen atoms were located from the Fourier maps and refined anisotropically. All the hydrogen atoms were put on calculated positions or located from the Fourier maps and refined isotropically with the isotropic vibration parameters related to the non-H atom to which they are bonded. Crystallographic and refinement details are listed in Table 1. The selected bond lengths and angles for compounds **1** and **3** are given in Tables 2 and 3, respectively.

CCDC 775840 and 775841 contain the supplementary crystallographic data for this paper. These data can be obtained free of charge at www.ccdc.cam.ac.uk/conts/retrieving.html [or from the Cambridge Crystallographic Data Center, 12 Union Road, Cambridge CB2 1EZ, UK; fax: (Internet) +44 1223 336 033; e-mail: deposit@ccdc.cam.ac.uk].

Table 1
Crystallographic data for **1** and **3**.

Compounds	**1**	**3**
Empirical formula	$C_{14}H_{32}N_2O_{14}P_4Zn_3$	$C_{19}H_{36}Co_2N_3O_{13}P_4$
F_w	772.41	756.25
Crystal system	Monoclinic	Monoclinic
Space group	$C2/c$	$P2_1/c$
a (Å)	36.326(10)	5.629 (18)
b (Å)	6.464 (18)	18.673(7)
c (Å)	11.183(3)	27.932(10)
β (deg)	94.43 (5)	100.98(9)
V (Å^3)	2618.3(12)	2882.6(18)
Z	4	4
d_{calcd} (g cm^3)	1.949	1.743
$F(000)$	1568	1556
Goodness of-fit on F^2	1.078	1.078
R_1, wR_2 [$I > 2\sigma(I)$][a]	0.0502, 0.1146	0.0472, 0.1058
R_1, wR_2 (all data)[a]	0.0638, 0.1178	0.0810, 0.1129
$(\Delta\rho)_{max}$, $(\Delta\rho)_{min}$ (e Å^3)	0.518, −1.032	0.429, −0.731

[a] $R_1 = \Sigma||F_o| - |F_c||/\Sigma|F_o|$, $wR_2 = [\Sigma w(F_o^2 - F_c^2)^2/\Sigma w(F_o^2)^2]^{1/2}$.

Table 2
Selected bond lengths (Å) and angles (deg) for **1**.[a]

Zn(1)–O(1)	1.945(3)	Zn(1)–O(4)	1.963(3)
Zn(2)–O(3)	2.026(4)	Zn(2)–O(5)	2.046(4)
Zn(2)–O(1W)	2.068(3)	Zn(2)–O(1B)	2.459(3)
Zn(2)–O(2B)	2.073(4)	Zn(2)–O(6C)	2.088(4)
P(1)–O(2)	1.507(4)	P(1)–O(1)	1.512(3)
P(1)–O(3)	1.512(4)	P(2)–O(4)	1.519(3)
P(2)–O(5)	1.512(4)	P(2)–O(6)	1.504(4)
O(1)–Zn(1)–O(1A)	127.5(2)	O(1)–Zn(1)–O(4A)	117.43(15)
O(1)–Zn(1)–O(4)	96.93(14)	O(4A)–Zn(1)–O(4)	97.8(2)
O(3)–Zn(2)–O(5)	95.25(14)	O(3)–Zn(2)–O(1W)	92.24(14)
O(5)–Zn(2)–O(1W)	91.78(14)	O(3)–Zn(2)–O(2B)	114.53(14)
O(5)–Zn(2)–O(2B)	86.64(14)	O(1W)–Zn(2)–O(2B)	153.22(14)
O(3)–Zn(2)–O(6C)	93.19(14)	O(5)–Zn(2)–O(6C)	170.67(14)
O(1W)–Zn(2)–O(6C)	91.88(13)	O(2B)–Zn(2)–O(6C)	86.22(13)
O(3)–Zn(2)–O(1B)	177.07(14)	O(5)–Zn(2)–O(1B)	82.04(12)
O(1W)–Zn(2)–O(1B)	88.96(12)	O(2B)–Zn(2)–O(1B)	64.33(13)
O(6C)–Zn(2)–O(1B)	89.44(13)	Zn(1)–O(1)–Zn(2D)	133.01(16)
P(2)–O(4)–Zn(1)	121.8(2)	P(1)–O(3)–Zn(2)	126.7(2)
P(1)–O(1)–Zn(1)	133.4(2)	P(1)–O(1)–Zn(2D)	86.32(15)
P(1)–O(2)–Zn(2D)	101.88(18)	P(2)–O(5)–Zn(2)	136.6(2)
P(2)–O(6)–Zn(2D)	131.7(2)		

[a] Symmetry codes: A: $-x, y, -z+3/2$;B: $x, -y, z-1/2$; C: $x, y-1, z$; D: $x, -y, z+1/2$.

Table 3
Selected bond lengths (Å) and angles (deg) for **3**.[a]

Co(1)–O(10)	2.028(3)	Co(1)–O(3A)	2.028(3)
Co(1)–O(1)	2.057(3)	Co(1)–O(4)	2.061(3)
Co(1)–O(7)	2.181(3)	Co(2)–O(8B)	2.066(3)
Co(2)–O(2)	2.075(3)	Co(2)–O(5)	2.119(3)
Co(2)–O(11B)	2.134(3)	Co(2)–O(1W)	2.143(3)
Co(2)–N(3)	2.231(4)	P(1)–O(3)	1.511(3)
P(1)–O(2)	1.514(3)	P(1)–O(1)	1.531(3)
P(2)–O(5)	1.499(3)	P(2)–O(4)	1.522(3)
P(2)–O(6)	1.565(3)	P(3)–O(8)	1.498(3)
P(3)–O(7)	1.521(3)	P(3)–O(9)	1.577(3)
P(4)–O(12)	1.503(3)	P(4)–O(10)	1.541(3)
P(4)–O(11)	1.546(3)		
O(10)–Co(1)–O(3A)	92.06(11)	O(10)–Co(1)–O(1)	92.79(12)
O(3A)–Co(1)–O(1)	101.82(11)	O(10)–Co(1)–O(4)	172.38(12)
O(3A)–Co(1)–O(4)	88.23(11)	O(1)–Co(1)–O(4)	94.61(12)
O(10)–Co(1)–O(7)	92.52(11)	O(3A)–Co(1)–O(7)	168.87(11)
O(1)–Co(1)–O(7)	88.09(11)	O(4)–Co(1)–O(7)	85.90(11)
O(8B) –Co(2)–O(2)	175.03(12)	O(8B)–Co(2)–O(5)	92.09(11)
O(2)–Co(2)–O(5)	92.88(11)	O(8B)–Co(2)–O(11B)	85.19(11)
O(2)–Co(2)–O(11B)	95.27(11)	O(5)–Co(2)–O(11B)	87.19(11)
O(8B)–Co(2)–O(1W)	87.98(12)	O(2)–Co(2)–O(1W)	92.45(12)
O(5)–Co(2)–O(1W)	82.57(11)	O(11B)–Co(2)–O(1W)	167.47(12)
O(8B)–Co(2)–N(3)	85.00(11)	O(2)–Co(2)–N(3)	90.06(12)
O(5)–Co(2)–N(3)	170.60(12)	O(11B)–Co(2)–N(3)	101.43(12)
O(1W)–Co(2)–N(3)	88.39(12)	P(1)–O(1)–Co(1)	134.79(17)
P(1)–O(2)–Co(2)	122.22(17)	P(1)–O(3)–Co(1C)	155.62(18)
P(2)–O(4)–Co(1)	119.75(18)	P(2)–O(5)–Co(2)	137.64(17)
P(3)–O(7)–Co(1)	134.37(17)	P(3)–O(8)–Co(2D)	127.75(16)
P(4)–O(10)–Co(1)	124.69(16)	P(4)–O(11)–Co(2D)	127.94(17)

[a] Symmetry codes: A: $x-1, y, z$; B: $-x+1, y+1/2, -z+3/2$; C: $x+1, y, z$; D: $-x+1, y-1/2, -z+3/2$.

3. Results and discussions

3.1. Syntheses

Compounds **1–4** have been synthesized by the reactions of metal salts with $cmdpH_4$ and 4,4′-bipyridine under hydrothermal conditions. The pH and the reaction temperature are found to play important roles in the composition and purity of the final products. Compound **1** can be obtained as a pure phase in different yields when the reaction mixture (molar ratio Zn:$cmdpH_4$=1:1) is adjusted to pH 2.0–3.0 and heated at 120–160 °C for 3 days. A lower pH (<2.0) results in a clear solution, while a higher pH (>3.0) leads to a flocculent mixture. For compound **2**, a pure phase can be obtained only at pH 3.5–4.0. Pure phases of **3** and **4** with good crystal quality and high yield can be obtained through hydrothermal reactions of $CoSO_4 \cdot 7H_2O$ or $MnSO_4 \cdot H_2O$, $cmdpH_4$ and 4, 4′-bipyridine (molar ratio=1:1:1) at 180 °C in the pH range of 3.0–3.5. The lower reaction temperature (160 °C) leads to the same crystalline products but with a lower yield and together with some unrecognized floccule-like materials. Attempts to prepare the suitable single crystals of compounds **2** and **4** for structural determination were unsuccessful. We have also carried out similar reactions by using other transition metal (Fe, Cu and Ni) salts or lanthanide salts as starting materials. Unfortunately, only flocculent mixture or powder phase are obtained, and their XRD patterns are different from those of **1–4**.

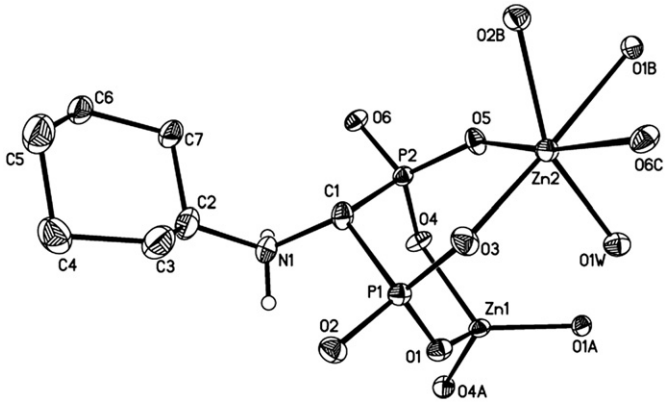

Fig. 1. Building unit of compound **1** (thermal ellipsoids shown at 30% probability). All hydrogen atoms attached to C atoms and the water molecule are omitted for clarity. Symmetry codes: A: $-x, y, -z+3/2$; B: $x, -y, z-1/2$; C: $x, y-1, z$.

3.2. Description of structures *1* and *2*

Compounds **1** and **2** are isostructural according to their XRD patterns (Fig. S1, supporting information). Compound **1** is structurally determined. It crystallizes in monoclinic space group $C2/c$. The asymmetric unit consists of 1.5 Zn atoms, one $cmdpH^{3-}$ ligand and one coordinated water molecule (Fig. 1). Zn(1) locates at a special position (0.00, 0.2525 and 0.75) and has a tetrahedral geometry. The four coordination sites are provided by phosphonate oxygen atoms [O(1), O(4), O(1A), O(4A)] from two equivalent $cmdpH^{3-}$ ligands. Zn(2) resides at a general position, and displays a distorted octahedral coordination environment. The six sites are filled with phosphonate oxygen atoms [O(3), O(5), O(1B), O(2B), O(6C)] from three $cmdpH^{3-}$ ligands and one water molecule [O(1W)]. The Zn–O bond lengths fall in the range of 1.945(3)–2.459(3) Å. The Zn–O–Zn bond angles are between 64.34(12)° and 177.07(13)°.

The $cmdpH^{3-}$ acts as a zwitterionic hepta-dentate ligand with the amino group protonated (Scheme 2b). Each $cmdpH^{3-}$ is linked to three Zn(2) atoms through corner- or edge-sharing of $\{Zn(2)O_6\}$ octahedra and $\{PO_3C\}$ tetrahedra and vice-versa, forming a single layer containing 3- and 7-member rings (Fig. 2a). The Zn(2)···Zn(2) distances across the O–P–O units within the single layer are 5.773(2) and 6.465(2) Å. Each $cmdpH^{3-}$ also bis-chelates and bridges Zn(1) and Zn(2) atoms through O(1), O(4), O(3) and O(5) atoms, thus leading to a novel double layer structure in which single layers of Zn(2)–PO_3 are pillared by $\{Zn(1)O_4\}$ tetrahedra. The Zn(1)···Zn(2) distances are 4.044(1) Å across the μ_3–O(1) and 4.199(1) and 5.390(1) Å over the O–P–O bridges (Fig. 2). The layers are packed along the a-axis with the cyclohexylamine groups filling in the interlayer spaces through van der Waals interactions (Fig. 3). The interlayer distance is ca. 18.6 Å (0.5a). As far as we are aware, such a

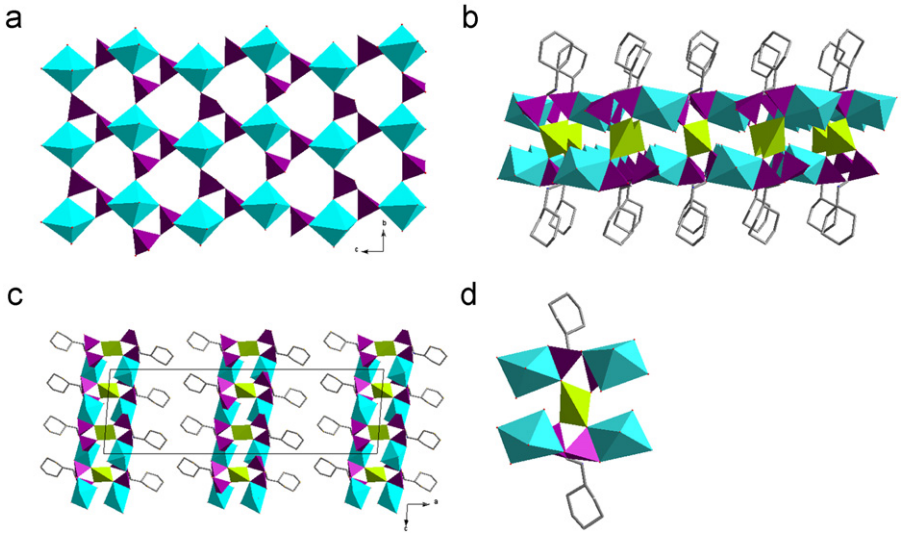

Fig. 2. Polyhedral representation of structure **1**: (a) the Zn(2)–PO_3 inorganic single layer; (b) the double layer; (c) packing diagram along the b-axis and (d) the Zn connection within the double layer. Color codes: $Zn(2)O_6$ cyan, $Zn(1)O_4$ green, PO_3C purple (for interpretation of the references to color in this figure legend, the reader is referred to the web version of this article).

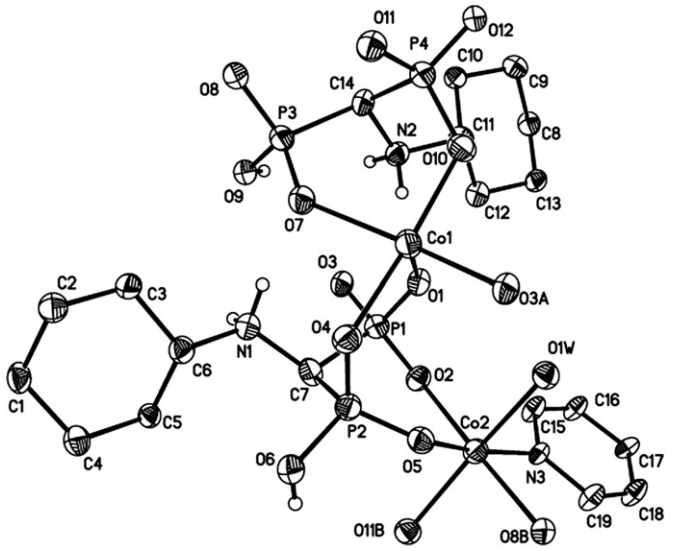

Fig. 3. Building unit of compound **3** (thermal ellipsoids shown at 30% probability). All hydrogen atoms attached to C atoms and the water molecule are omitted for clarity. Symmetry codes: A: $x-1, y, z$; B: $-x+1, y+1/2, -z+3/2$.

double layer structure has not been documented in the literature for metal phosphonates.

3.3. Description of structures *3* and *4*

Compounds **3** and **4** are also isostructural based on their XRD patterns (Fig. S2, supporting information). Compound **3** is structurally determined. It crystallizes in monoclinic space group $P2_1/c$. The asymmetric unit is composed of two Co atoms, two $cmdpH_2^{2-}$ ligands, 0.5 4,4′-bipyridine and one coordination water molecule (Fig. 3). The Co(1) atom is coordinated by five phosphonate oxygen atoms [O(1), O(4), O(7), O(10), O(3A)] from three $cmdpH_2^{2-}$ ligands, displaying a distorted tetragonal pyramidal geometry. The Co(1)–O bond lengths are between 2.028(3) and 2.181(3) Å. The Co(2) atom is octahedrally coordinated by four phosphonate oxygen atoms [O(2), O(5), O(8B), O(11B)], one water [O(1W)] and one nitrogen [N(3)] from 4,4′-bipyridine. The Co(2)–O(N) bond distances fall in the range of 2.066(3)–2.231(3) Å, in agreement with those in the other cobalt phosphonate compounds [28,35–42].

There are two crystallographically distinguished $cmdpH_2^{2-}$ ligands in structure **3**. Each $cmdpH_2^{2-}$, with the amino nitrogen and one phosphonate oxygen atoms protonated, bis-chelates and bridges Co(1) and Co(2) atoms by using its four phosphonate oxygen atoms [O(1), O(2), O(4) and O(5) for type I; O(7), O(8), O(10) and O(11) for type II] (Scheme 2c and d), forming an infinite chain running along the *b*-axis. The Co(1)···Co(2) distances across the O–P–O bridges within the chain are 4.811(2) and 5.181(2) Å. The adjacent chains are further linked by O(1)–P(1)–O(3) units through Co(1) atoms, resulting in an inorganic layer in the *ab* plane which contains 3- and 10-member rings (Fig. 4). The Co(1)···Co(1) distance over the O–P–O bridge is 5.630 Å. These layers are pillared by 4,4′-bipyridine via coordination with the Co(2) atoms from neighboring layers, leading to an open framework structure with channels generated along the *a*-axis. The channel size is ca. 18.6×11.5 Å (van der Waals radii not accounted) (Fig. 4). The channel size is slightly larger than that found in compound $Co_3[HO_2C(C_6H_4)CH_2N(CH_2PO_3H)(CH_2PO_3)]_2(4,4'\text{-bipy})(H_2O)_4$ in which a pillared layer architecture is also found [43]. The cyclohexylamine moieties locate within the channels. Extensive hydrogen-bonding interactions are found among the amino groups, phosphonate oxygen atoms and coordination water molecules. The shortest contacts are 2.953 Å for O(1W)···O(2^{i}), 2.459 Å for O(6)···O(12^{ii}), 2.852 Å for O(9)···O(10^{iii}), 2.760 Å for N(1)···O(4^{iii}), 2.773 Å for N(1)···O(7) and 2.799 Å for N(2)···O(10^{iii}) (symmetry codes: i: $x-1, y, z$; ii: $-x+1, y+1/2, -z+3/2$; iii: $x+1, y, z$).

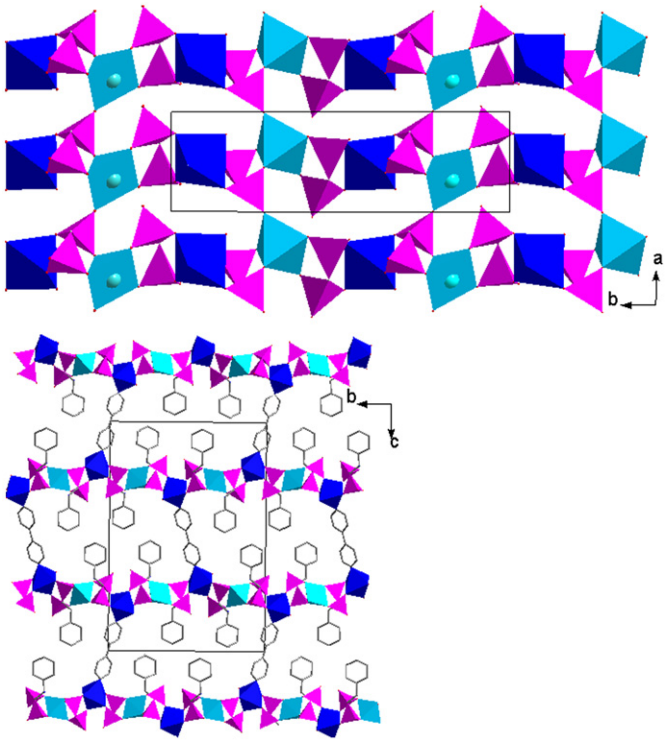

Fig. 4. Polyhedral representation of structure **3**. Top: the inorganic layer; bottom: packing diagram along the *a*-axis. Color codes: $Co(2)NO_5$ blue, $Co(1)O_5$ sky blue, PO_3C purple (for interpretation of the references to color in this figure legend, the reader is referred to the web version of this article).

Structures **1–4** are obviously different from those of the other metal phosphonates based on $(R_1)(R_2)NCH(PO_3H_2)_2$ such as compound $Na_4Zn\{NH_3CH(PO_3)_2\}_2 \cdot 4H_2O$ containing Zn–PO_3 chains, compound $Ni\{NH_3CH(PO_3H)_2\}_2 \cdot xH_2O$ with a square-grid layer structure [29], and compound $NaCo_2\{NH_3CH(PO_3)(PO_3H_{0.5})\}_2(H_2O)_2 \cdot xH_2O$ in which the Co–PO_3 layer contains 4- and 8-member rings [28]. Apparently, the introduction of a flexible cyclohexyl group into the iminomethylenediphosphonate and the incorporation of a second 4,4′-bipy coligand lead to the formation of metal phosphonates with novel architectures.

3.4. Magnetic properties

The temperature-dependent magnetic susceptibility data of compounds **2–4** were measured in the temperature range 1.8–300 K under 2 kOe. For compound **2**, the effective magnetic moment per Co_3 unit at 300 K is 8.26μ_B, higher than the spin only value for spin $S=3/2$ centers ($g=2$, 6.71μ_B), attributed to the significant orbital contribution of the octahedral Co(II) ions [32]. Upon cooling down from room temperature, the decreasing of the $\chi_M T$ value and the appearance of the maximum in the χ_M versus T plot show dominant antiferromagnetic interactions between Co(II) centers (Fig. 5). The antiferromagnetic interaction is confirmed by the negative Weiss constant ($\theta = -31.6$ K), determined by the Curie–Weiss fit of the magnetic susceptibility data above 50 K.

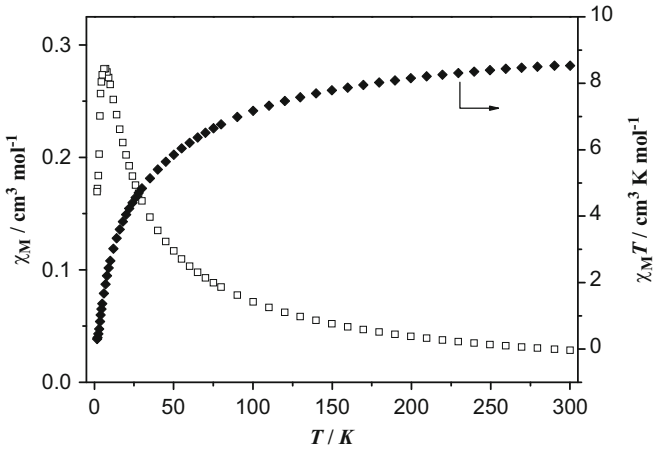

Fig. 5. The χ_M and $\chi_M T$ versus T plots for compound **2.**

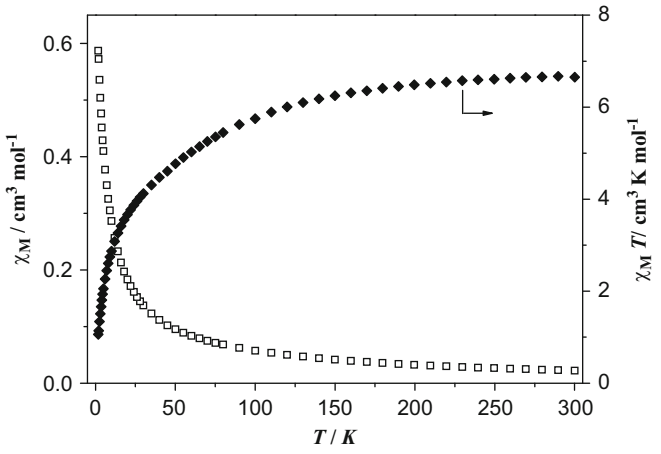

Fig. 7. The χ_M and $\chi_M T$ versus T plots for compound **3**.

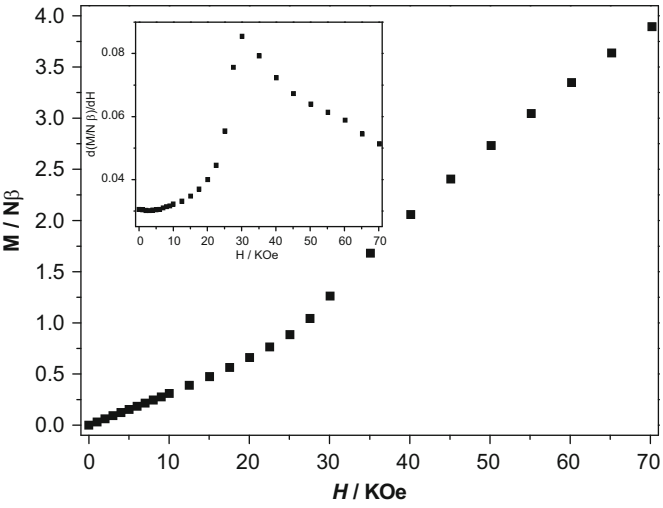

Fig. 6. Field-dependent magnetization for compound **2** at 1.8 K. Inset: The dM/dH versus H curve.

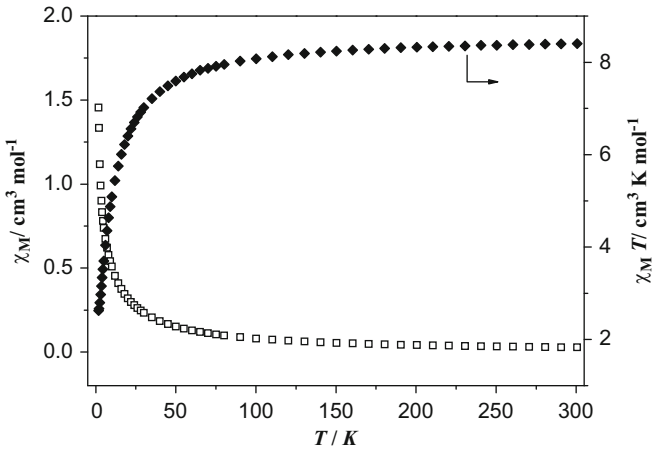

Fig. 8. The χ_M and $\chi_M T$ versus T plots for compound **4**.

According to its structure, the magnetic exchanges between the Co(II) ions may be propagated through both μ_3–O and O–P–O bridges within the layer. Considering that the Co(1)···Co(2) distance across the μ_3–O(1) could be shorter than that via the O–P–O (according to structure **1**), we tried to fit the magnetic data using a trimer model based on Hamiltonian $H=-2J\Sigma S_i S_j$. The effort was, however, not successful. The isothermal field dependence of magnetization at 1.8 K is shown in Fig. 6. The magnetization increases gradually with increasing external field and displays an inflexion at about 30 kOe, determined by the peak in the dM/dH plot, showing a characteristic of a spin flop behavior. The magnetization at 70 kOe is 3.89$N\beta$ which is far from the saturation value for three Co(II).

Fig. 7 shows the χ_M and $\chi_M T$ versus T plots for compound **3**. At 300 K, the effective magnetic moment per Co_2 unit (7.29μ_B) is higher than the expected spin only value for $S=3/2$ ($g=2$, 5.48μ_B), attributed to the orbital contribution of Co(II) ion. The Curie–Weiss fit of the susceptibility data in the temperature range of 50–300 K gives a θ of -26.5 K. This negative Weiss constant together with the continuous decreasing of $\chi_M T$ value upon cooling indicate that antiferromagnetic coupling could dominate between the Co(II) ions besides the spin–orbital coupling of the single Co(II) ions. Fig. 8 shows the χ_M and $\chi_M T$ versus T plots for compound **4**. The effective magnetic moment at room temperature is 8.2μ_B per Mn_2 unit, close to the expected spin only value (8.36μ_B) for spin $S=5/2$ and $g=2$. The decreasing of $\chi_M T$ upon cooling indicates an antiferromagnetic interaction between the magnetic centers. In the temperature range 50–300 K, the magnetic behavior follows the Curie–Weiss law with a Weiss constant of -6.3 K. The negative Weiss constant also confirms the antiferromagnetic exchange between the Mn(II) ions.

4. Conclusions

This paper reports four metal diphosphonate compounds **1–4** based on *N*-cyclohexylaminomethanediphosphonate. Compounds $Zn_3(cmdpH)_2(H_2O)_2$ (**1**) and $Co_3(cmdpH)_2(H_2O)_2$ (**2**) are isostructural. They show a novel double-layer structure in which the single layers of $M(2)$–PO_3 are pillared by $M(1)O_4$ tetrahedra. The incorporation of 4,4′-bipyridine leads to the formation of isostructural compounds $Co_2(cmdpH_2)_2(4,4'\text{-bipy})_{0.5}(H_2O)$ (**3**) and $Mn_2(cmdpH_2)_2(4,4'\text{-bipy})_{0.5}(H_2O)$ (**4**). Both exhibit a pillared layered structure in which the inorganic layers made up of corner-sharing $Co(1)O_5$ tetragonal pyramids, $Co(2)NO_5$ octahedra and PO_3C tetrahedra are pillared by 4,4′-bipyridine. Dominant antiferromagnetic interactions are found in compounds **2–4** and an interesting spin flop behavior is observed in compound **2**. Further work is in progress to explore new metal phosphonate materials with new architectures and interesting physical properties.

Acknowledgments

This work was supported by NSFC (no. 90922006), the National Basic Research Program of China (nos. 2007CB925102, 2010CB923402), NSF of Jiangsu Province (no. BK2009009) and NSFC for Creative Research Group (no. 20721002). We thank Prof. You Song and Dr. Tian-Wei Wang for magnetic measurements.

Appendix A. Supplementary material

Supplementary data associated with this article can be found in the online version at doi:10.1016/j.jssc.2010.05.008.

References

[1] V.V. Krishnan, A.G. Dokoutchaev, M.E. Thompson, J. Catal. 196 (2000) 366–374.
[2] C. Maillet, P. Janvier, M. Pipeplier, T. Praveen, Y. Andres, B. Bujoli, Chem. Mater. 13 (2001) 2879–2884.
[3] A. Hu, G.T. Yee, W. Lin, J. Am. Chem. Soc. 127 (2005) 12486–12487.
[4] S.S. Bao, L.F. Ma, Y. Wang, L. Fang, C.J. Zhu, Y.Z. Li, L.M. Zheng, Chem. Eur. J. 13 (2007) 2333–2343.
[5] A. Clearfield, Dalton Trans. (2008) 6089–6102.
[6] Z. Wang, G. Chen, K. Ding, Chem. Rev. 109 (2009) 322–359.
[7] A. Hamada, P. Braunstein, Inorg. Chem. 48 (2009) 1624–1637.
[8] J.G. Mao, Coord. Chem. Rev. 251 (2007) 1493–1520.
[9] L. Cunha-Silva, S. Lima, D. Ananias, P. Silva, L. Mafra, L.D. Carlos, M. Pillinger, A.A. Valente, F.A.A. Paz, J. Rocha, J. Mater. Chem. 19 (2009) 2618–2632.
[10] A. Clearfield, Prog. Inorg. Chem. 47 (1998) 371–510.
[11] K. Maeda, Microporous Mesoporous Mater. 73 (2004) 47–55.
[12] J.A. Groves, S.R. Miller, S.J. Warrender, C. Mellot Draznieks, P. Lightfoot P.A. Wright, Chem. Commun. (2006) 3305–3307.
[13] J. Wu, H. Hou, H. Han, Y. Fan, Inorg. Chem. 46 (2007) 7960–7970.
[14] S.R. Miller, G.M. Pearce, P.A. Wright, F. Bonino, S. Chavan, S. Bordiga I. Margiolaki, N. Guillou, G. Férey, S. Bourryelly, P.L. Llewellyn, J. Am. Chem. Soc. 130 (2008) 15967–15981.
[15] T.Y. Ma, X.J. Zhang, Z.Y. Yuan, Microporous Mesoporous Mater. 123 (2009) 234–242.
[16] D. Cave, F.C. Coomer, E. Molinos, H.H. Klauss, P.T. Wood, Angew. Chem. Int. Ed. 45 (2006) 803–806.
[17] M. Shanmugam, G. Chastanet, T. Mallah, R. Sessoli, S.J. Teat, G.A. Timco, R.E.P. Winpenny, Chem. Eur. J. 12 (2006) 8777–8785.
[18] J.T. Brockman, T.C. Stamatatos, W. Wernsdorfer, K.A. Abboud, G. Christou, Inorg. Chem. 46 (2007) 9160–9171.
[19] S. Khanra, M. Kloth, H. Mansaray, C.A. Muryn, F. Tuna, E.C. Sanudo M. Helliwell, E.J.L. McInnes, R.E.P. Winpenny, Angew. Chem. Int. Ed. 46 (2007) 5568–5571.
[20] Y.S. Ma, Y.Z. Li, Y. Song, L.M. Zheng, Inorg. Chem. 47 (2008) 4536–4544.
[21] J.T. Li, T.D. Keene, D.K. Cao, S. Decurtins, L.M. Zheng, Cryst. Eng. Commun. 11 (2009) 1255–1260.
[22] D.E. Hughes, M. Mian, D.F. Guilland-Cumming, R.G.G. Russel, Drugs Exp. Clin. Res. 17 (1991) 109–114.
[23] G.A. Rondan, T.J. Martin, Science 289 (2000) 1508–1514.
[24] L. Widler, K.A. Jaeggi, M. Glatt, K. Müller, R. Bachmann, M. Bisping, A. Ruth Born, R. Cortesi, G. Guiglia, H. Jeker, U. Ramseier, J. Schmid, G. Schreiber. Y. Seltenmeyer, J.R. Green, J. Med. Chem. 45 (2002) 3721–3738.
[25] E. Matczak-Jon, V. Videnova-Adrabińska, A. Burzyńska, P. Kafarski, T. Lis, Chem. Eur. J. 11 (2005) 2357–2372.
[26] E. Matczak-Jon, V. Videnova-Adrabinska, Coord. Chem. Rev. 249 (2005) 2458–2488.
[27] U. Kortz, M.T. Pope, Inorg. Chem. 34 (1995) 3848–3850.
[28] S.S. Bao, L.M. Zheng, Y.J. Liu, W. Xu, S.H. Feng., Inorg. Chem. 42 (2003) 5037–5039.
[29] S.S. Bao, T.W. Wang, Y.Z. Li, L.M. Zheng, J. Solid State Chem. 179 (2006) 413–420.
[30] S.F. Tang, J.L. Song, X.L. Li, J.G. Mao, Cryst. Growth Des. 7 (2007) 360–366.
[31] M. Wu, R. Chen, Y. Huang, Synth. Commun. 34 (2004) 1393–1398.
[32] O. Kahn, in: Molecular Magnetism, VCH Publishers, Inc., New York, 1993.
[33] SAINT, Program for Data Extraction and Reduction, Siemens Analytical X-ray Instruments, Madison, WI, 1994–1996.
[34] SHELXTL (version 5.0), Reference Manual, Siemens Industrial Automation, Analytical Instruments, Madison, WI, 1997.
[35] D.K. Cao, Y.Z. Li, L.M. Zheng, Inorg. Chem. 46 (2007) 7571–7578.
[36] D.G. Ding, B.L. Wu, Y.T. Fan, H.W. Hou, Cryst. Growth Des. 9 (2009) 508–516.
[37] T.H. Yang, Y. Liao, L.M. Zheng, R.E. Dinnebier, Y.H. Su, J. Ma, Chem. Commun. (2009) 3023–3025.
[38] B.P. Yang, A.V. Prosvirin, Y.Q. Guo, J.G. Mao, Inorg. Chem. 47 (2008) 1453–1459.
[39] A.V. Palii, O.S. Reu, S.M. Ostrovsky, S.I. Klokishner, B.S. Tsukerblat, Z.M. Sun, J.G. Mao, A.V. Prosvirin, H.H. Zhao, K.R. Dunbar, J. Am. Chem. Soc. 130 (2008) 14729–14738.
[40] T.O. Salami, X. Fan, P.Y. Zavalij, S.R.J. Oliver, Dalton Trans. (2006) 1574–1578.
[41] H. Li, G.S. Zhu, X.D. Guo, F.X. Sun, H. Ren, Y. Chen, S.L. Qiu, Eur. J. Inorg. Chem. (2006) 4123–4128.
[42] S. Bauer, T. Bein, N. Stock, Inorg. Chem. 44 (2005) 5882–5889.
[43] J.L. Song, A.V. Prosvirin, H.H. Zhao, J.G. Mao, Eur. J. Inorg. Chem. (2004) 3706–3711.